

Theoretical and experimental study on synchronization of the two homodromy excitors in a non-resonant vibrating system

Xue-Liang Zhang*, Chun-Yu Zhao and Bang-Chun Wen

School of Mechanical Engineering and Automation, Northeastern University, Shenyang, Liaoning, China

Received 14 April 2012

Revised 28 September 2012

Accepted 3 October 2012

Abstract. In this paper we give some theoretical analyses and experimental results on synchronization of the two non-identical excitors. Using the average method of modified small parameters, the dimensionless coupling equation of the two excitors is deduced. The synchronization criterion for the two excitors is derived as the torque of frequency capture being equal to or greater than the absolute value of difference between the residual electromagnetic torques of the two motors. The stability criterion of synchronous state is verified to satisfy the Routh-Hurwitz criterion. The regions of implementing synchronization and that of stability of phase difference for the two excitors are manifested by numeric method. Synchronization of the two excitors stems from the coupling dynamic characteristic of the vibrating system having selecting motion, especially, under the condition that the parameters of system are complete symmetry, the torque of frequency capture stemming from the circular motion of the rigid frame drives the phase difference to approach PI and carry out the swing of the rigid frame; that from the swing of the rigid frame forces the phase difference to near zero and achieve the circular motion of the rigid frame. In the steady state, the motion of rigid frame will be one of three types: pure swing, pure circular motion, swing and circular motion coexistence. The numeric and experiment results derived thereof show that the two excitors can operate synchronously as long as the structural parameters of system satisfy the criterion of stability in the regions of frequency capture. In engineering, the distance between the centroid of the rigid frame and the rotational centre of exciter should be as far as possible. Only in this way, can the elliptical motion of system required in engineering be realized.

Keywords: Synchronization, vibrating system, stability, vibratory synchronization transmission

1. Introduction

In the natural world, human society, or fields of engineering and technology, the synchronous phenomena or synchronous problems can be found everywhere. The earliest detailed accounts on synchronized motion was made by Huygens [1]. Since 1894, the synchronous phenomena was also found in nonlinear circuits by scientists, such as Rayleigh [2] found that two organ tubes could produce a synchronized sound when the outlets are close to each other, and Pol [3] observed the synchronization of certain electrical-mechanical system. They called this phenomena as “frequency capture”. “Frequency capture” or “synchronization”, therefore, is a unique phenomenon of nonlinear system. In the 1960s, Blekhman [4–10] in Soviet Union proposed the synchronization theory of mechanical excitors. Chinese scholar Prof. Wen, applied such synchronization theory to engineering and established a branch of vibration

*Corresponding author: Xue-Liang Zhang, School of Mechanical Engineering and Automation, Northeastern University, Shenyang 110004, Liaoning, China. E-mail: luckyzx17788@163.com.

utilization engineering [11–15]. Balthazar [16] has also given some short comments on self-synchronization of two non-ideal sources by means of numerical simulations. Many theories of synchronization of more than two excitors are studied by scholars, in which the main methods used are the method of direct motion separation [4–10] and the averaging method of small parameters [17–20]. In Refs. [17–19] synchronization of the two non-identical excitors with rotating oppositely in a non-resonant vibrating system of plane motion was investigated, and that of the two excitors of spatial motion was also discussed in Ref. [20]. In this paper, synchronization of the two Homodromy excitors is studied by using the average method of modified small parameters. We present that the vibrating system driven by the two excitors has the coupling dynamic characteristic of selecting motion, and the theory method used is verified to be feasible and descriptive by experiment.

This paper contains the following elements: The dynamic model and motion equations of system are given firstly. The criterion of implementing frequency capture and that of stability of the synchronous state are deduced by followed. Next section, a quantitative numeric discussions are provided. Experiments are given in Section 5. Finally, concludes this paper.

2. The dynamic model and motion equations of system

The dynamic model of the considered vibrating system is illustrated in Fig. 1. Springs are connected to a rigid frame. The two induction motors, are supplied with the same electrical source at the same time, and installed symmetrically in the rigid frame, rotate in the same directions and drive two eccentric lumps (two excitors) to excite the vibrating system. The frame oxy is a fixed frame, and its origin o is the equilibrium point of centroid of the rigid frame. The motions of the rigid frame are vibrations in x - and y -directions, denoted by x and y , and swing about its centroid, denoted by ψ . Each eccentric lump rotates about its spin axis, denoted by φ_i , $i = 1, 2$. Using Lagrange's equations, and choosing the x, y, ψ, φ_1 , and φ_2 as the generalized coordinates, we derive the differential equations of motion of the vibrating system in the form:

$$\begin{aligned} M\ddot{x} + f_x\dot{x} + k_x x &= m_1 r_1 (\dot{\varphi}_1^2 \cos \varphi_1 + \ddot{\varphi}_1 \sin \varphi_1) + m_2 r_2 (\dot{\varphi}_2^2 \cos \varphi_2 + \ddot{\varphi}_2 \sin \varphi_2) \\ M\ddot{y} + f_y\dot{y} + k_y y &= m_1 r_1 (\dot{\varphi}_1^2 \sin \varphi_1 - \ddot{\varphi}_1 \cos \varphi_1) + m_2 r_2 (\dot{\varphi}_2^2 \sin \varphi_2 - \ddot{\varphi}_2 \cos \varphi_2) \\ J\ddot{\psi} + f_\psi\dot{\psi} + k_\psi\psi &= m_1 r_1 l_0 [\dot{\varphi}_1^2 \sin(\varphi_1 - \beta) - \ddot{\varphi}_1 \cos(\varphi_1 - \beta)] \\ &\quad - m_2 r_2 l_0 [\dot{\varphi}_2^2 \sin(\varphi_2 + \beta) - \ddot{\varphi}_2 \cos(\varphi_2 + \beta)] \\ J_{01}\ddot{\varphi}_1 + f_1\dot{\varphi}_1 &= T_{e1} - m_1 r_1 [\ddot{y} \cos \varphi_1 - \ddot{x} \sin \varphi_1 + l_0 \ddot{\psi} \cos(\varphi_1 - \beta) + l_0 \dot{\psi}^2 \sin(\varphi_1 - \beta)] \\ J_{02}\ddot{\varphi}_2 + f_2\dot{\varphi}_2 &= T_{e2} - m_2 r_2 [\ddot{y} \cos \varphi_2 - \ddot{x} \sin \varphi_2 - l_0 \ddot{\psi} \cos(\varphi_2 + \beta) - l_0 \dot{\psi}^2 \sin(\varphi_2 + \beta)] \end{aligned} \quad (1)$$

where

$$M = m + \sum_{i=1}^2 m_i, \quad J = (m + m_1 + m_2)l_e^2, \quad f_\psi = \frac{1}{2}(f_x l_y^2 + f_y l_x^2), \quad k_\psi = \frac{1}{2}(k_y l_x^2 + k_x l_y^2), \quad J_{0j} = m_i r^2 + j_{oj}.$$

m is the mass of the rigid frame; m_i the mass of the exciter i , $i = 1, 2$; l_0 the distance between the rotational centre o_i of the exciter- i and the mass centre o of the rigid frame; $r_1 = r_2 = r$ the eccentric radius of two eccentric lumps; β the angle between $o_1 o$ and x -axis; β_1 the angle between Ao and x -axis; k_x, k_y and k_ψ the constants of springs, and f_x, f_y and f_ψ the damping constants in x -, y - and ψ -directions, respectively; f_j the damping constant of rotor of the motor j and J_{0j} its moment of inertia; j_{oj} the moment of inertia of motor- oj axis which can be neglected, $j = 1, 2$; l_e the equivalent rotating radius of the vibrating system about the centroid of the rigid frame; T_{ej} the electromagnetic torque of the motor j . (\bullet) and $(\ddot{\bullet})$ signify $d \bullet / dt$ and $d^2 \bullet / dt^2$, respectively.

3. Frequency capture of the two excitors and stability of synchronous state

As illustrated in Fig. 1, assuming the average phase of the two excitors and their phase difference to be φ and 2α , respectively, then we obtain

$$\varphi_1 = \varphi + \alpha, \varphi_2 = \varphi - \alpha \quad (2)$$

The average mechanical angular velocity of the two excitors therefore, is $\dot{\varphi}$. Due to the periodical motion of the vibrating system, the mechanical angular velocities of the two motors change periodically. If the least common multiple period of the two motors is assumed to be T_{LCMP} , the average value of their average angular velocity over time T_{LCMP} , then must be a constant, i.e.

$$\omega_{m0} = \frac{1}{T_{LCMP}} \int_{t'}^{t' + T_{LCMP}} \dot{\varphi}(t) dt = \text{constant} \quad (3)$$

Assuming the instantaneous change coefficients of $\dot{\varphi}$ and $\dot{\alpha}$ to be ε_1 and ε_2 (ε_1 and ε_2 are the functions of time t), i.e., $\dot{\varphi} = (1 + \varepsilon_1) \omega_{m0}$, $\dot{\alpha} = \varepsilon_2 \omega_{m0}$, respectively, we have

$$\begin{aligned} \dot{\varphi}_1 &= (1 + \varepsilon_1 + \varepsilon_2) \omega_{m0} = (1 + \nu_1) \omega_{m0}, \quad \nu_1 = \varepsilon_1 + \varepsilon_2 \\ \dot{\varphi}_2 &= (1 + \varepsilon_1 - \varepsilon_2) \omega_{m0} = (1 + \nu_2) \omega_{m0}, \quad \nu_2 = \varepsilon_1 - \varepsilon_2 \end{aligned} \quad (4)$$

The two excitors can operate synchronously, if the average values of ε_1 and ε_2 over the single period ($T_0 = 2\pi/\omega_{m0}$) are zero, i.e., $\bar{\varepsilon}_1 = 0$ and $\bar{\varepsilon}_2 = 0$. Generally in engineering, the masses of eccentric lumps are far smaller than that of the rigid frame [11–14], the coupling terms of $\dot{\psi}$ in the first two formulae of Eq. (1) and that of \ddot{x} and \ddot{y} in the third formula, therefore, have been neglected. On the other hand, the slip of an induction motor usually ranges from 2% to 8% [21], i.e., $\dot{\varepsilon}_1 \ll 1$ and $\dot{\varepsilon}_2 \ll 1$, so $\dot{\varphi}_1$ and $\dot{\varphi}_2$ can be neglected in the first three formulae of Eq. (1) when the vibrating system operates in the steady-state. We assume m_1 is m_0 and m_2 is ηm_0 ($0 < \eta \leq 1$), and Eq. (4) are inserted into the first three formulae of Eq. (1) to yield

$$\begin{aligned} M\ddot{x} + f_x\dot{x} + k_x x &= m_0 r \omega_{m0}^2 [(1 + \varepsilon_1 + \varepsilon_2)^2 \cos(\varphi + \alpha) + \eta(1 + \varepsilon_1 - \varepsilon_2)^2 \cos(\varphi - \alpha)] \\ M\ddot{y} + f_y\dot{y} + k_y y &= m_0 r \omega_{m0}^2 [(1 + \varepsilon_1 + \varepsilon_2)^2 \sin(\varphi + \alpha) + \eta(1 + \varepsilon_1 - \varepsilon_2)^2 \sin(\varphi - \alpha)] \\ J\ddot{\psi} + f_\psi\dot{\psi} + k_\psi\psi &= m_0 r \omega_{m0}^2 l_0 [(1 + \varepsilon_1 + \varepsilon_2)^2 \sin(\varphi + \alpha - \beta) - \eta(1 + \varepsilon_1 - \varepsilon_2)^2 \sin(\varphi - \alpha - \beta)] \end{aligned} \quad (5)$$

For a non-resonant machinery, the operating frequency of system is about (3~10) times of its natural frequency and the damping constants of springs are very small [11–14] according to Ref. [17], the responses of Eq. (5) can be expressed in the form:

$$\begin{aligned} x &= -\frac{r_m r}{\mu_x} [\cos(\varphi + \alpha + \gamma_x) + \eta \cos(\varphi - \alpha + \gamma_x)], \\ y &= -\frac{r_m r}{\mu_y} [\sin(\varphi + \alpha + \gamma_y) + \eta \sin(\varphi - \alpha + \gamma_y)], \\ \psi &= -\frac{r_m r r_l}{l_e \mu_\psi} [\sin(\varphi + \alpha - \beta + \gamma_\psi) - \eta \sin(\varphi - \alpha + \beta + \gamma_\psi)]. \end{aligned} \quad (6)$$

where

$$\begin{aligned} r_m &= \frac{m_0}{M}, \quad l_e = \sqrt{\frac{J}{M}}, \quad r_l = \frac{l_0}{l_e}, \quad \mu_x = 1 - \frac{\omega_{nx}^2}{\omega_{m0}^2}, \quad \mu_y = 1 - \frac{\omega_{ny}^2}{\omega_{m0}^2}, \quad \mu_\psi = 1 - \frac{\omega_{n\psi}^2}{\omega_{m0}^2}, \quad \omega_{nx} = \sqrt{\frac{k_x}{M}}, \\ \omega_{ny} &= \sqrt{\frac{k_y}{M}}, \quad \omega_{n\psi} = \sqrt{\frac{k_\psi}{J}}, \quad \gamma_i = \frac{2\xi_{ni}(\omega_{ni}/\omega_{m0})}{1 - (\omega_{ni}/\omega_{m0})^2}, \quad i = x, y, \psi \end{aligned}$$

ξ_{nx} , ξ_{ny} and $\xi_{n\psi}$ are the damping ratios of springs ($\xi_{nx} \leq 0.07$, $\xi_{ny} \leq 0.07$ and $\xi_{n\psi} \leq 0.07$) [11,12], $\pi - \gamma_i$, denotes the phase angle in i -direction, $i = x, y, \psi$.

Differentiating x , y and ψ in Eq. (6) with respect to time t by the chain rule, respectively, we obtain \ddot{x} , \ddot{y} and $\ddot{\psi}$, which are inserted into the last two formulae of Eq. (1) and integrating them over $\varphi = 0 \sim 2\pi$, and neglecting the highorder terms of ε_1 and ε_2 , the balanced equations of the two exciters are expressed as

$$\begin{aligned} J_{01}\omega_{m0}(\dot{\bar{\varepsilon}}_1 + \dot{\bar{\varepsilon}}_2) + f_1\omega_{m0}(1 + \bar{\varepsilon}_1 + \bar{\varepsilon}_2) &= T_{e1} - \bar{T}_{L1} \\ J_{02}\omega_{m0}(\dot{\bar{\varepsilon}}_1 - \dot{\bar{\varepsilon}}_2) + f_2\omega_{m0}(1 + \bar{\varepsilon}_1 - \bar{\varepsilon}_2) &= T_{e2} - \bar{T}_{L2} \end{aligned} \quad (7)$$

with

$$\begin{aligned} \bar{T}_{L1} &= \chi'_{11}\dot{\bar{\varepsilon}}_1 + \chi'_{12}\dot{\bar{\varepsilon}}_2 + \chi_{11}\bar{\varepsilon}_1 + \chi_{12}\bar{\varepsilon}_2 + \chi_a + \chi_{f1} \\ \bar{T}_{L2} &= \chi'_{21}\dot{\bar{\varepsilon}}_1 + \chi'_{22}\dot{\bar{\varepsilon}}_2 + \chi_{21}\bar{\varepsilon}_1 + \chi_{22}\bar{\varepsilon}_2 - \chi_a + \chi_{f2} \end{aligned} \quad (8)$$

where

$$\begin{aligned} \chi'_{11} &= m_0 r^2 \omega_{m0} [-W_{c0} - W_s \sin(2\alpha + \theta_s) + W_c \cos(2\alpha + \theta_c)]/2, \\ \chi'_{12} &= m_0 r^2 \omega_{m0} [-W_{c0} + W_s \sin(2\alpha + \theta_s) - W_c \cos(2\alpha + \theta_c)]/2, \\ \chi'_{21} &= m_0 r^2 \omega_{m0} [-\eta^2 W_{c0} + W_s \sin(2\alpha + \theta_s) + W_c \cos(2\alpha + \theta_c)]/2, \\ \chi'_{22} &= m_0 r^2 \omega_{m0} [\eta^2 W_{c0} + W_s \sin(2\alpha + \theta_s) + W_c \cos(2\alpha + \theta_c)]/2, \\ \chi_{11} &= m_0 r^2 \omega_{m0}^2 [W_{s0} + W_s \cos(2\alpha + \theta_s) + W_c \sin(2\alpha + \theta_c)], \\ \chi_{12} &= m_0 r^2 \omega_{m0}^2 [W_{s0} - W_s \cos(2\alpha + \theta_s) - W_c \sin(2\alpha + \theta_c)], \\ \chi_{21} &= m_0 r^2 \omega_{m0}^2 [\eta^2 W_{s0} + W_s \cos(2\alpha + \theta_s) - W_c \sin(2\alpha + \theta_c)], \\ \chi_{22} &= m_0 r^2 \omega_{m0}^2 [-\eta^2 W_{s0} + W_s \cos(2\alpha + \theta_s) - W_c \sin(2\alpha + \theta_c)], \\ \chi_{f1} &= m_0 r^2 \omega_{m0}^2 [W_{s0} + W_s \cos(2\alpha + \theta_s)]/2, \\ \chi_{f2} &= m_0 r^2 \omega_{m0}^2 [\eta^2 W_{s0} + W_s \cos(2\alpha + \theta_s)]/2, \\ \chi_a &= m_0 r^2 \omega_{m0}^2 W_c \sin(2\alpha + \theta_c)/2, \quad W_{s0} = r_m \left(\frac{\sin \gamma_x}{\mu_x} + \frac{\sin \gamma_y}{\mu_y} + \frac{r_l^2 \sin \gamma_\psi}{\mu_\psi} \right), \\ W_{c0} &= r_m \left(\frac{\cos \gamma_x}{\mu_x} + \frac{\cos \gamma_y}{\mu_y} + \frac{r_l^2 \cos \gamma_\psi}{\mu_\psi} \right), \\ W_s &= \eta r_m \sqrt{a_s^2 + b_s^2}, \quad \theta_s = \begin{cases} \arctan(-b_s/a_s), & a_s \geq 0 \\ \pi + \arctan(-b_s/a_s), & a_s < 0 \end{cases}, \quad W_c = \eta r_m \sqrt{a_c^2 + b_c^2}, \\ \theta_c &= \begin{cases} \arctan(b_c/a_c), & a_c \geq 0 \\ \pi + \arctan(b_c/a_c), & a_c < 0 \end{cases}, \\ a_s &= \frac{\sin \gamma_x}{\mu_x} + \frac{\sin \gamma_y}{\mu_y} - \frac{r_l^2 \sin \gamma_\psi}{\mu_\psi} \cos(2\beta), \quad b_s = -\frac{r_l^2 \sin \gamma_\psi}{\mu_\psi} \sin(2\beta), \\ a_c &= -\frac{\cos \gamma_x}{\mu_x} - \frac{\cos \gamma_y}{\mu_y} + \frac{r_l^2 \cos \gamma_\psi}{\mu_\psi} \cos(2\beta), \quad b_c = -\frac{r_l^2 \cos \gamma_\psi}{\mu_\psi} \sin(2\beta). \end{aligned}$$

Compared with the change of φ ($\dot{\varphi} = \omega_{m0}$) with respect to time t , that of ε_1 , ε_2 , $\dot{\varepsilon}_1$ and $\dot{\varepsilon}_2$ are very small. ε_1 and ε_2 , therefore, are considered to be slow-changing parameters, while the change of φ is considered as fast-changing parameter, in this study. According to the method of direct separation of motions [4–10], ε_1 , ε_2 , $\dot{\varepsilon}_1$, $\dot{\varepsilon}_2$ and α are

assumed to be the middle values of their integrations $\bar{\varepsilon}_1$, $\bar{\varepsilon}_2$, $\dot{\bar{\varepsilon}}_1$, $\dot{\bar{\varepsilon}}_2$ and $\bar{\alpha}$ respectively during the aforementioned integration.

If the two motors are supplied with the same electric source and have identical pole pairs, their electromagnetic torques can be expressed as follows:

$$T_{e1} = T_{e01} - k_{e01}(\bar{\varepsilon}_1 + \bar{\varepsilon}_2), \quad T_{e2} = T_{e02} - k_{e02}(\bar{\varepsilon}_1 - \bar{\varepsilon}_2) \quad (9)$$

where T_{e01} and T_{e02} are the electromagnetic torques, k_{e01} and k_{e02} the stiffness of angular velocity when the two motors operate at the angular velocity of ω_{m0} [20].

We choose exciter 1 as the standard exciter ($m_1 = m_0, m_2 = \eta m_0, 0 < \eta \leq 1$) to normalize Eq. (7) in the following manner: firstly substituting Eqs (8) and (9) into Eq. (7), and then dividing Eq. (7) by the moment of the standard exciter, $m_0 r^2 \omega_{m0}$, after that, adding two formulae as the first row, subtracting the second formula from the first one as the second row, next introducing the non-dimensional parameters $\rho_1, \rho_2, \kappa_1, \kappa_2$, and $\bar{\nu}_1, \bar{\nu}_2$

$$\rho_1 = 1 - W_{c0}/2, \quad \rho_2 = \eta - \eta^2 W_{c0}/2, \quad \bar{\nu}_1 = \bar{\varepsilon}_1 + \bar{\varepsilon}_2, \quad \bar{\nu}_2 = \bar{\varepsilon}_1 - \bar{\varepsilon}_2$$

$$\kappa_1 = k_{e01}/(m_0 r^2 \omega_{m0}^2) + f_1/(m_0 r \omega_{m0}) + W_{s0}, \quad \kappa_2 = k_{e02}/(m_0 r^2 \omega_{m0}^2) + f_2/(m_0 r^2 \omega_{m0}) + \eta^2 W_{s0},$$

and finally writing them into the matrix form, frequency capture equation of the two excitors can be expressed in the form:

$$A\dot{\nu} = B\nu + u \quad (10)$$

where

$$\begin{aligned} \nu &= \{\bar{\nu}_1, \bar{\nu}_2\}^T, \quad u = \{u_1, u_2\}^T, \\ a_{11} &= \rho_1 + \rho_2 + W_c \cos(2\bar{\alpha} + \theta_c), \quad a_{12} = \rho_1 - \rho_2 + W_s \cos(2\bar{\alpha} + \theta_s), \\ a_{21} &= \rho_1 - \rho_2 - W_s \sin(2\bar{\alpha} + \theta_s), \quad a_{22} = \rho_1 + \rho_2 - W_c \cos(2\bar{\alpha} + \theta_c), \\ b_{11} &= -\omega_{m0}(\kappa_1 + \kappa_2 - 2W_s \cos(2\bar{\alpha} + \theta_s)), \quad b_{12} = -\omega_{m0}(\kappa_1 - \kappa_2 - 2W_c \sin(2\bar{\alpha} + \theta_c)), \\ b_{21} &= -\omega_{m0}(\kappa_1 - \kappa_2 + 2W_c \sin(2\bar{\alpha} + \theta_c)), \quad b_{22} = -\omega_{m0}(\kappa_1 + \kappa_2 + 2W_s \cos(2\bar{\alpha} + \theta_s)), \\ u_1 &= [T_{e01}/(m_0 r^2 \omega_{m0}) - f_1/(m_0 r^2)] + [T_{e02}/(m_0 r^2 \omega_{m0}) - f_2/(m_0 r^2)] - \omega_{m0} W_{s0}(1 + \eta^2)/2 \\ &\quad - \omega_{m0} W_s \cos(2\bar{\alpha} + \theta_s), \\ u_2 &= [T_{e01}/(m_0 r^2 \omega_{m0}) - f_1/(m_0 r^2)] - [T_{e02}/(m_0 r^2 \omega_{m0}) - f_2/(m_0 r^2)] - \omega_{m0} W_{s0}(1 - \eta^2)/2 \\ &\quad - \omega_{m0} W_c \sin(2\bar{\alpha} + \theta_c). \end{aligned}$$

Equation (10) describes the coupling relation of the two excitors and is referred to as the dimensionless coupling equation of the two excitors.

3.1. The criterion of implementing frequency capture

Substituting $\bar{\nu}_1 = 0$ and $\bar{\nu}_2 = 0$ into Eq. (10), we have $u_1 = 0$ and $u_2 = 0$. Calculating the sum and the difference of u_1 and u_2 , and rearranging them as following

$$T_{e01} + T_{e02} - (f_1 + f_2)\omega_{m0} - [m_0 r^2 \omega_{m0}^2 W_{s0}(1 + \eta^2)/2 + m_0 r^2 \omega_{m0}^2 W_s \cos(2\bar{\alpha} + \theta_s)] = 0 \quad (11)$$

$$(T_{e01} - T_{e02}) - (f_1 - f_2)\omega_{m0} - m_0 r^2 \omega_{m0}^2 W_{s0}(1 - \eta^2)/2 = m_0 r^2 \omega_{m0}^2 W_c \sin(2\bar{\alpha} + \theta_c) \quad (12)$$

In the above Eq. (11), $T_{e01} + T_{e02}$ is the sum of electromagnetic torques of the two motors; $(f_1 + f_2)\omega_{m0}$ is that of the rotors damping torques of the two motors; the last terms, $\chi_{f1} + \chi_{f2}$, is the sum of the load torques that the

vibrating system acts on the two motors. Equation (11), therefore, is the equation of torque balance of the vibrating system operating in the steady-state.

Rewriting Eq. (12), we have

$$\sin(2\bar{\alpha} + \theta_c) = T_D/T_C, \quad 2\bar{\alpha} = \arcsin(T_D/T_C) - \theta_c \quad (13)$$

where

$$T_C = m_0 r^2 \omega_{m0}^2 W_c, \quad T_D = T_{R1} - T_{R2}, \quad T_{R1} = T_{e01} - f_1 \omega_{m0} - m_0 r^2 \omega_{m0}^2 W_{s0}/2,$$

$$T_{R2} = T_{e02} - f_2 \omega_{m0} - m_0 r^2 \omega_{m0}^2 \eta^2 W_{s0}/2.$$

T_C is the torque of frequency capture; T_D the difference between the residual electromagnetic torques of the two motors; T_{R1} and T_{R2} the residual electromagnetic torques of the motors 1 and 2, respectively.

Since $|\sin(2\bar{\alpha} + \theta_c)| \leq 1$, the criterion of implementing vibration synchronization is

$$T_C \geq |T_D| \quad (14)$$

Equation (14) indicates that the criterion of synchronization for the two excitors is that the torque of frequency capture is equal to or greater than the absolute value of difference between the residual electromagnetic torques of the two motors.

Equations (11) and (12) are nonlinear functions of ω_{m0} and $\bar{\alpha}$, their solutions, ω_{m0}^* and $\bar{\alpha}_0$, can be determined by numeric method.

3.2. Stability of synchronous state

Linearizing Eq. (10) around $\bar{\alpha} = \bar{\alpha}_0$ and appending the third row, $\Delta\dot{\alpha} = \omega_{m0}^* \bar{\varepsilon}_2$ ($\Delta\alpha = \bar{\alpha} - \bar{\alpha}_0$), after that, writing them as a system of the three first-order differential equations, and using the notation $\mathbf{z} = \{\varsigma_1 \varsigma_2 \Delta\alpha\}$ yields

$$\dot{\mathbf{z}} = \mathbf{A}'^{-1} \mathbf{B}' \mathbf{z} \quad (15)$$

where

$$\mathbf{z} = \{\bar{\varepsilon}_1 + \bar{\varepsilon}_2, \bar{\varepsilon}_1 - \bar{\varepsilon}_2, \bar{\alpha} - \bar{\alpha}_0\}^T, \quad \mathbf{A}' = \begin{bmatrix} a'_{11} & a'_{12} & 0 \\ a'_{21} & a'_{22} & 0 \\ 0 & 0 & 1 \end{bmatrix}, \quad \mathbf{B}' = \begin{bmatrix} b'_{11} & b'_{12} & -2\omega_{m0}^* W_s \sin(2\bar{\alpha}_0 + \theta_s) \\ b'_{21} & b'_{22} & 2\omega_{m0}^* W_c \cos(2\bar{\alpha}_0 + \theta_c) \\ 0 & \omega_{m0}^* & 0 \end{bmatrix}.$$

It should be noted that, a'_{ij} and b'_{ij} denote the values of a_{ij} and b_{ij} in matrix \mathbf{A} and \mathbf{B} for $\bar{\alpha} = \bar{\alpha}_0$ and $\omega_{m0} = \omega_{m0}^*$.

Exponential time-dependence of the form $\dot{\mathbf{z}} = u \exp(\lambda t)$ is now assumed, and inserted into Eq. (15). Solving the determinant equation $\det(\mathbf{A}'^{-1} \mathbf{B}' - \lambda \mathbf{I}) = 0$, we deduce the characteristic equation for eigenvalue λ

$$\lambda^3 + c_1 \lambda^2 + c_2 \lambda + c_3 = 0 \quad (16)$$

where $c_1 = 4\omega_{m0}^* H_1/H_0$, $c_2 = 2\omega_{m0}^{*2} H_2/H_0$, $c_3 = 2\omega_{m0}^{*3} H_3/H_0$

$$\begin{aligned} H_0 &= 4\rho_1 \rho_2 - W_c^2 \cos^2(2\bar{\alpha}_0 + \theta_c) + W_s^2 \sin^2(2\bar{\alpha}_0 + \theta_s), \quad H_1 = \rho_1 \kappa_2 + \rho_2 \kappa_1 - W_s W_c \cos(\theta_c - \theta_s), \\ H_2 &= 2\kappa_1 \kappa_2 + (\rho_1 + \rho_2) W_c \cos(2\bar{\alpha}_0 + \theta_c) + (\rho_1 - \rho_2) W_s \sin(2\bar{\alpha}_0 + \theta_s) - W_s^2 \\ &\quad - W_s^2 \sin^2(2\bar{\alpha}_0 + \theta_s) + W_c^2 + W_c^2 \cos^2(2\bar{\alpha}_0 + \theta_c), \\ H_3 &= (\kappa_1 + \kappa_2) W_c \cos(2\bar{\alpha}_0 + \theta_c) + (\kappa_1 - \kappa_2) W_s \sin(2\bar{\alpha}_0 + \theta_s) + 2W_s W_c \cos(\theta_c - \theta_s). \end{aligned} \quad (17)$$

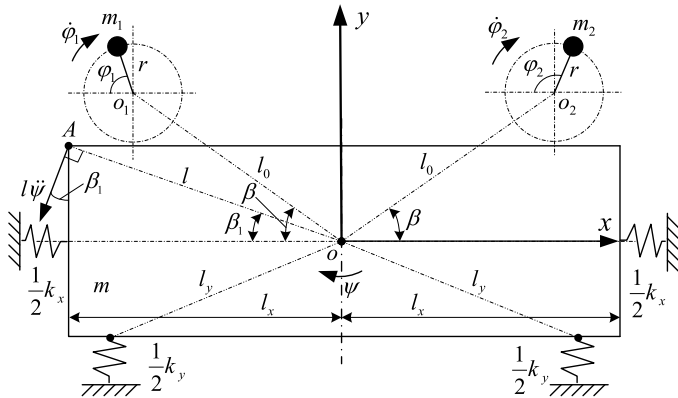
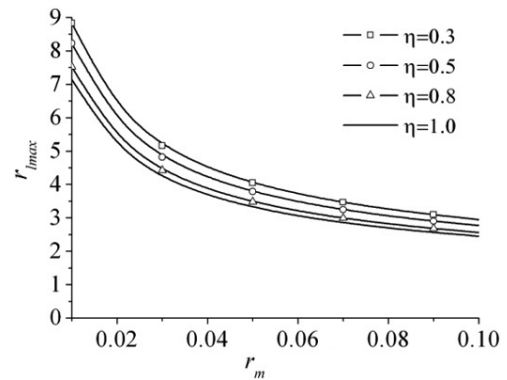


Fig. 1. Dynamic model of a vibrating system with the two homodromy excitors.

Fig. 2. The maximum of r_l^2 .

In engineering, compared with W_c in the expression of c_1, c_2 and c_3 , W_s is so small that it can be neglected [17–20]. H_0, H_1, H_2 and H_3 , then, can be simplified as:

$$\begin{aligned} H'_0 &= 4\rho_1\rho_2 - W_c^2 \cos^2(2\bar{\alpha}_0 + \theta_c), \quad H'_1 = \rho_1\kappa_2 + \rho_2\kappa_1, \\ H'_2 &= 2\kappa_1\kappa_2 + (\rho_1 + \rho_2)W_c \cos(2\bar{\alpha}_0 + \theta_c) + W_c^2 + W_c^2 \cos^2(2\bar{\alpha}_0 + \theta_c), \\ H'_3 &= (\kappa_1 + \kappa_2)W_c \cos(2\bar{\alpha}_0 + \theta_c). \end{aligned} \quad (18)$$

Based on the Routh-Hurwitz criterion [23], it can be seen that if and only if all roots of λ in Eq. (16) have the negative real part, i.e., Eq. (19) is satisfied, the zero solution of Eq. (15), $z = 0$, is stable. It should be noted that, since the two motors having the identical rated speed are supplied with the same electric source, the difference between the two motors' speed is the rather small. Furthermore, due to the periodical rotations of the two motors, and based on the method of direct separation of motions by averaging, when the time $t \rightarrow +\infty$, Eq. (19) can guarantee that the synchronous state of the vibrating system caused by the torque of frequency capture is stable, i.e., $\lim_{t \rightarrow +\infty} z = 0$ means $\lim_{t \rightarrow +\infty} \varepsilon_i = 0$ and $\lim_{t \rightarrow +\infty} \nu_i = 0$, $i = 1, 2$, we have $\lim_{t \rightarrow +\infty} \mathbf{A}\boldsymbol{\nu} = 0$.

$$c_1 > 0, c_3 > 0 \text{ and } c_1 c_2 > c_3 \quad (19)$$

According to the sign of H'_0 , Eq. (19) can be rewritten as Eqs (20) and (21)

$$H'_0 > 0, H'_1 > 0, H'_3 > 0 \text{ and } 4H'_1 H'_2 - H'_0 H'_3 > 0 \quad (20)$$

$$H'_0 < 0, H'_1 < 0, H'_3 < 0 \text{ and } 4H'_1 H'_2 - H'_0 H'_3 > 0 \quad (21)$$

From $H'_0 > 0$ and $H'_1 > 0$ ($\kappa_1 > 0$ and $\kappa_2 > 0$), we can deduce

$$\rho_1 > 0, \rho_2 > 0 \text{ and } 4\rho_1\rho_2 - W_c^2 \cos^2(2\bar{\alpha}_0 + \theta_c) > 0 \quad (22)$$

By $H'_3 > 0$, we obtain

$$\cos(2\bar{\alpha}_0 + \theta_c) > 0 \quad (23)$$

Inserting H'_0, H'_1, H'_2 and H'_3 into $4H'_1 H'_2 - H'_0 H'_3 > 0$ and rearranging it, we have

$$\begin{aligned} &[4\rho_1^2\kappa_2 + 4\rho_2^2\kappa_2 + (\kappa_1 + \kappa_2)W_c^2 \cos^2(2\bar{\alpha}_0 + \theta_c)]W_c \cos(2\bar{\alpha}_0 + \theta_c) > \\ &-4(\rho_1\kappa_2 + \rho_2\kappa_1)(2\kappa_1\kappa_2 + W_c^2 + W_c^2 \sin^2(2\bar{\alpha}_0 + \theta_c)) \end{aligned} \quad (24)$$

As shown in Eq. (24), if $\cos(2\bar{\alpha}_0 + \theta_c) > 0$, the left hand-side of Eq. (24) is greater than zero, and its right hand-side is less than zero when $\rho_1 > 0$ and $\rho_2 > 0$. Hence, Eqs (22) and (23) satisfy Eq. (24).

When $H'_0 < 0$, from $H'_1 < 0$, we have $\rho_1\kappa_2 + \rho_2\kappa_1 < 0$, and $H'_3 < 0$ requires $\cos(2\bar{\alpha}_0 + \theta_c) < 0$. In this case, the left hand-side of Eq. (24) is less than zero and its right hand-side is greater than zero. $H'_0 < 0, H'_1 < 0$ and $H'_3 < 0$ hence, can not meet the need of $4H'_1 H'_2 - H'_0 H'_3 > 0$.

Besides, one can see that, $2\bar{\alpha}_0 + \theta_c \in (-\pi/2, \pi/2)$ satisfies Eq. (23), from which the interval of $2\bar{\alpha}_0$ is determined by θ_c . Equations (22) and (23), therefore, are the stability criterions of synchronous states for the two excitors.

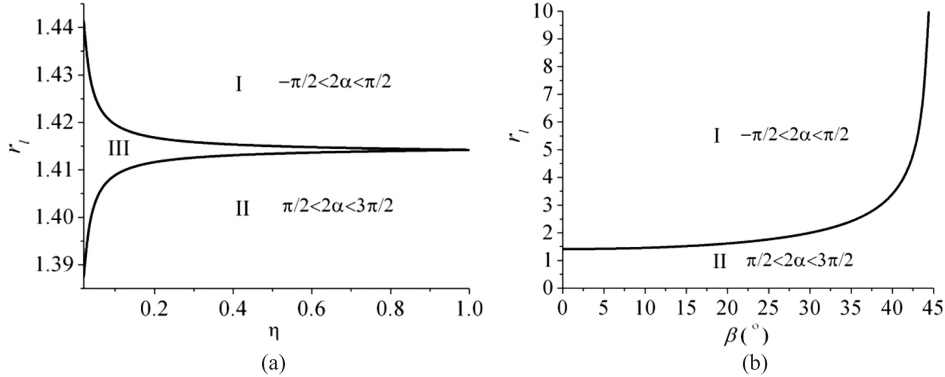


Fig. 3. Regions of frequency capture for the two identical motors: (a) $\beta = 0$; (b) $\beta \in (0, \pi/4]$.

4. Numeric discussions: The regions of frequency capture and characteristic of selecting motion

Section 3 has given some theoretical analyses in the simplified form on synchronization problem. This section will compare quantitatively the numeric results of the regions of frequency capture and the motion types of the vibrating system, with its above theoretically analytical results in the simplified form.

Based on the expression of r_l , its maximum can be simplified in the form

$$r_{l\max}^2 = \lim_{t_0 \rightarrow \infty} r_l^2 = \frac{1 + r_m(1 + \eta)}{r_m(1 + \eta)} \quad (25)$$

If $r_{l\max}^2$ satisfies Eqs (22) and (23), the synchronous state of system is always stable. As shown in Fig. 2, $r_{l\max} \approx 7$ for $\eta = 1$, the value of r_l can be arranged from 0 to 7 in the following discussions.

From Eq. (14), the main parameters that influence frequency capture of system are W_{s0} and W_c , which are functions of the dimensionless structural parameters r_m , r_l , η , u_x , u_y and u_ψ . In a non-resonant vibrating system, however, u_x , u_y and u_ψ change little (24/25–99/100) [11,12], we focus on investigating the effect of dimensionless parameters r_m , r_l , η on the frequency capture. To guarantee the torque of frequency capture, T_C in Eq. (13) should sufficiently overcome T_D , i.e., $T_C > |T_D|$. When the two identical motors are taken to drive the two non-identical unbalanced rotors, we have

$$T_D = T_{R1} - T_{R2} = -m_0 r^2 \omega_{m0}^2 W_{s0}(1 - \eta^2)/2 \quad (26)$$

Here, we assume that $T_{e01} - f_1 \omega_{m0} - (T_{e02} - f_2 \omega_{m0}) \approx 0$ just for convenient discussion (in engineering, actually, the difference between the electromagnetic torques of the two identical motors is not complete zero).

Equation (14), therefore, can be simplified in the form

$$W_c \geq -W_{s0}(1 - \eta^2)/2 \quad (27)$$

Figure 3(a) shows the regions of implementing frequency capture in ηr_l -plane for $\beta = 0$. From Eq. (27), r_m has no effect on the frequency capture. ηr_l -plane is divided into three Regions: I, II and III. The regions of implementing frequency capture are in Regions I and II, and the phase difference in the steady state is $2\alpha_0 \in (-\pi/2, \pi/2)$ in Region I, $2\alpha_0 \in (\pi/2, 3\pi/2)$ in Region II. The vibrating system can not implement frequency capture in Region III. Regions I, II and III converge into a point ($\eta = 1.0$, $r_l = 1.414 \approx \sqrt{2}$), at this point, $T_D = 0$, in other words, when the two motors are identical, this point is the best-matching parameters of the two excitors that can enhance the ability of the frequency capture.

Figure 3(b) shows the regions of the frequency capture with $\beta \neq 0$ ($\beta \in (0, \pi/4]$). Here, it is noteworthy that, η has little effect on the frequency capture by the fact that W_s is far smaller than W_c , i.e., Eq. (27) is always satisfied in Regions I and II.

Table 1
The motion types of the vibrating system

Parameters of vibrating system	$2\alpha_0$	Motion types of vibrating system
$\eta = 1.0$	$\beta = 0^\circ$ $r_l < \sqrt{2}$ (i.e., $a_c < 0$)	π Pure swing
	$r_l > \sqrt{2}$ (i.e., $a_c > 0$)	0 Circular motion
	$0^\circ < \beta < 90^\circ$	$(0, \pi)$ Swing and circular motion
	$\beta = 90^\circ$	π Pure swing
$\eta \neq 1.0$	$\beta = 0^\circ$ $r_l < \sqrt{2}$ (i.e., $a_c < 0$)	π Swing and circular motion
	$r_l > \sqrt{2}$ (i.e., $a_c > 0$)	0 Circular motion
	$0^\circ < \beta < 90^\circ$	$(0, \pi)$ Swing and circular motion
	$\beta = 90^\circ$	π Swing and circular motion

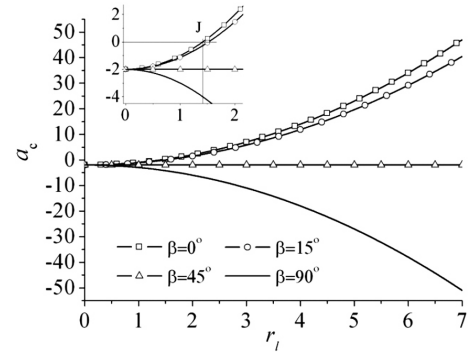


Fig. 4. The values of a_c for β and r_l .

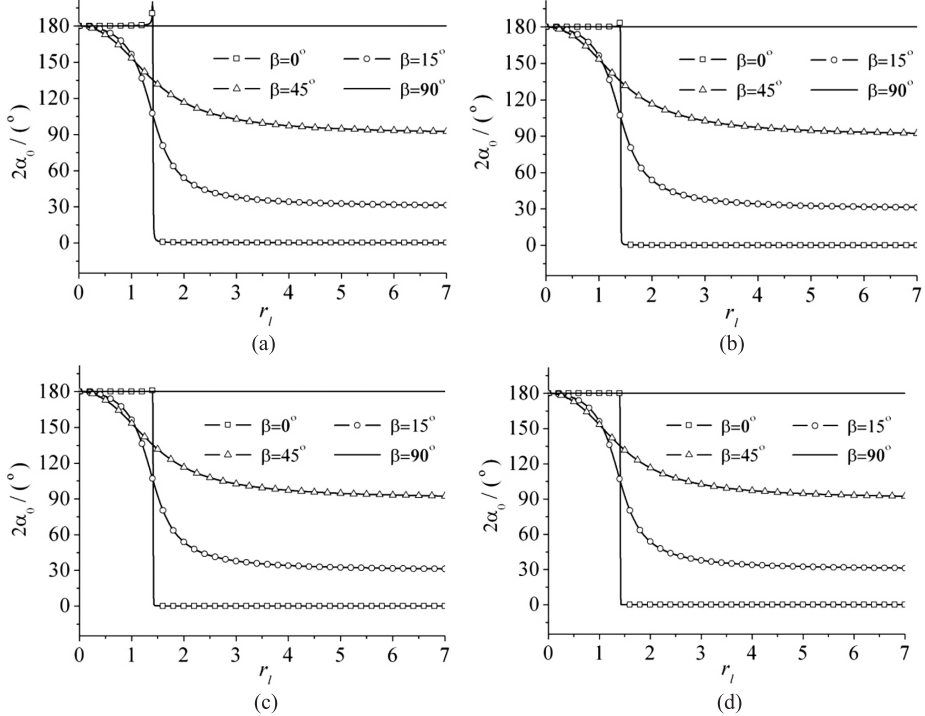


Fig. 5. Approximate values of $2\alpha_0$ with the two identical motors: (a) $\eta = 0.2$; (b) $\eta = 0.5$; (c) $\eta = 0.8$; (d) $\eta = 1.0$.

We assume that $\rho_C = T_C \sin(2\bar{\alpha} + \theta_c)/2$, if the structural parameters of system are Region I and II in Figs 3(a) and (b), from Eqs (11) and (12), we can see that, ρ_C acting on the phase-leading exciter is the load torque that limits the increase of its angular velocity. Meanwhile, it also acts on the other phase-lagging exciter, in which ρ_C is the driving torque that limits its the decrease of the angular velocity. Finally, the synchronous and stable operation of the two exciters is reached. When the two exciters operate in the steady state, the torque of frequency capture does no work.

When the two motors are identical, according to Eq. (13), the approximate values of $2\alpha_0$ for r_l , η and β are shown in Fig. 5.

Based on the sign of a_c and the value of $2\alpha_0$ in Figs 4 and 5, respectively, the motion types of the vibrating system are expressed in Table 1.

In Table 1, when the structural parameters of system are complete symmetry, i.e., $\eta = 1.0, \beta = 0^\circ$ ($W_c = \eta r_m |a_c|$), according to the expression of the torque of frequency capture, which is determined by a_c . In this case,

Table 2
The parameters of experimental system

Contents	Values
The mass of vibrating system: M (kg)	152
The moment of vibrating system: J ($\text{kg}\cdot\text{m}^2$)	17
The mass of standard eccentric lamp ($r = 0.05 \text{ m}$): m_0 (kg)	4
The constant of springs in x -direction: k_x (N/m)	77000
The constant of springs in y -direction: k_y (N/m)	77650
The constant of springs in ψ -direction: k_ψ (Nm/rad)	3000
The damping constant in x -directions: f_x (N/(m/s))	270
The damping constant in y -directions: f_y (N/(m/s))	270
The damping constant in ψ -directions: f_ψ (N/(m/s))	220

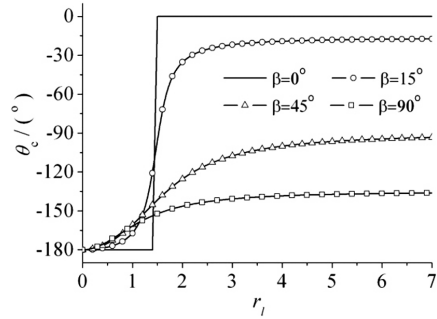


Fig. 6. The angle of the general dynamic symmetry.

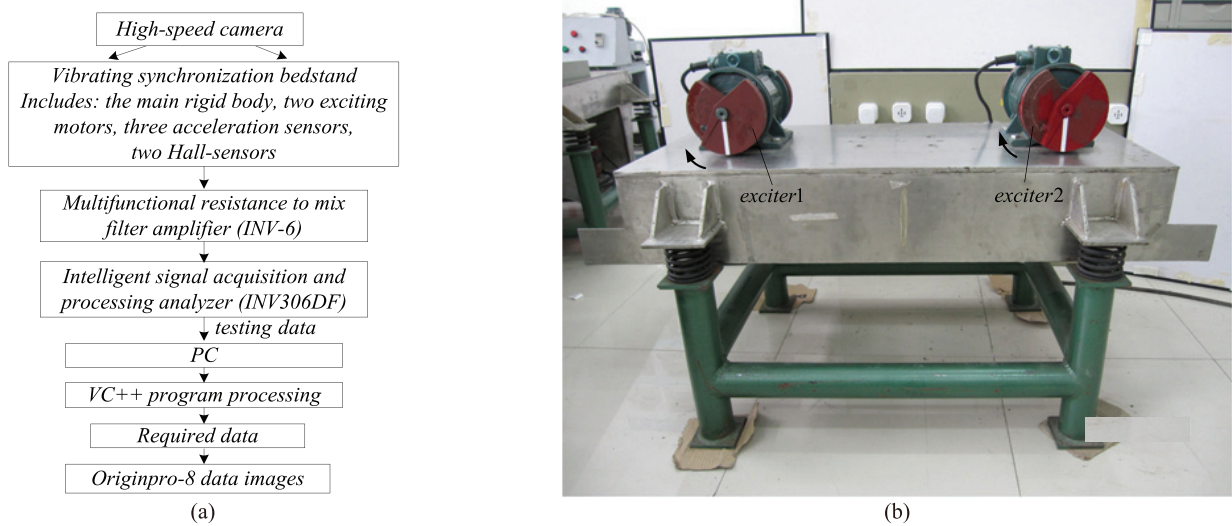


Fig. 7. A laboratory model of a vibrating system: (a) Schematic of experimental setup; (b) Vibrating synchronization bedstand.

the motions of the rigid frame excited by the two exciters are the circular motion (x - and y -directions) and the swing (ψ -direction) about its centroid. The torque of frequency capture resulting from the circular motion of the rigid frame drives the phase difference to approach π and implement the swing of the rigid frame; that from the swing of the rigid frame forces the phase difference to approach 0 and carry out the circular motion of the rigid frame. In the expression of a_c , the terms related to the circular motion of the rigid frame are negative, and that referred to the swing are positive. $a_c < 0$ (i.e., $r_l < \sqrt{2}$) means that the contribution of the circular motion on the ρ_C is greater than that of the swing, the vibrating system, thus, selects the swing of the rigid frame, vice versa.

When $\eta = 1.0$, $0^\circ < \beta < 90^\circ$, the torque of frequency capture is determined by a_c and b_c (b_c is related to the swing of rigid frame), in this case, the system shares the circular motion and the swing of the rigid frame. The phase difference of the two exciters and the motion types of rigid frame are shown in the relevant figures of Fig. 5 and Table 1.

If $\eta = 1.0$, $\beta = 90^\circ$, we have $a_c < 0$ (as shown in Fig. 4), the vibrating system still selects the swing of the rigid frame.

Under the condition of $\eta \neq 1.0$, the torque of frequency capture decreases to η ($0 < \eta < 1$) times of its original value. Based on the above principle discussed, the torque of frequency capture drives the phase difference to approach the corresponding value shown in Fig. 5. The motion types of the rigid frame are shown in Table 1, here, we do not discuss in more detail.

The above facts demonstrate that the vibrating system has the coupling dynamic characteristic of selecting motion. Under the case that the criterions of the frequency capture and that of the stability of the two excitors are all

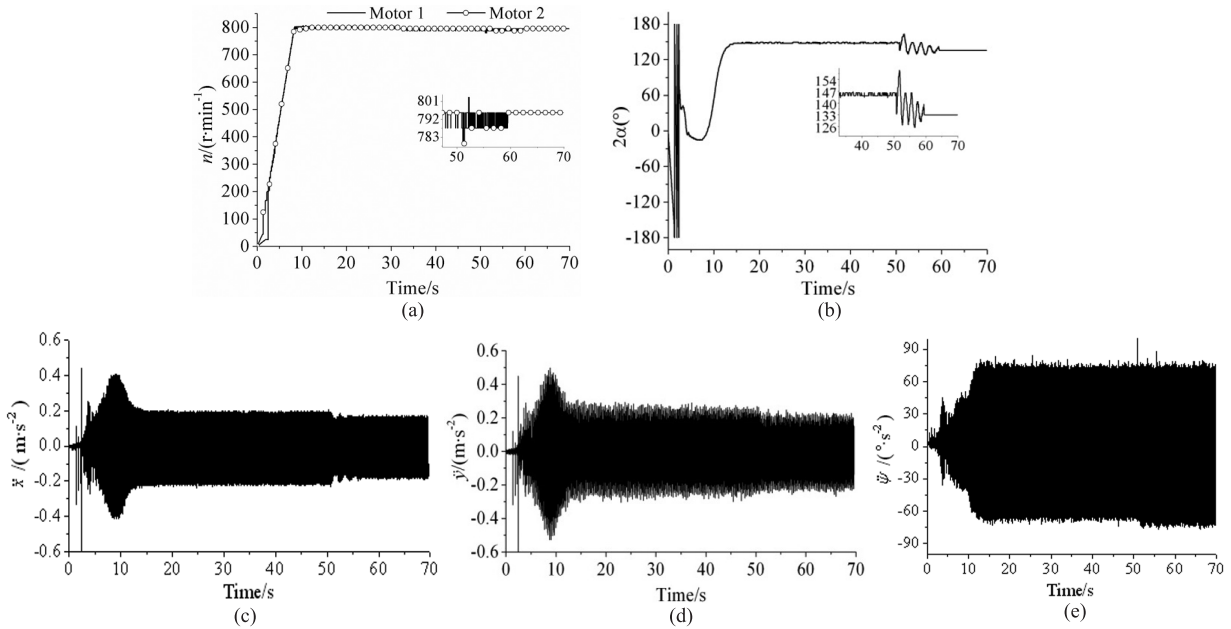


Fig. 8. The experimental results of the two non-identical excitors rotating in the same directions ($\eta = 0.5$): (a) Rotational velocities of the two excitors; (b) The phase difference between the two excitors ($2\alpha = \varphi_1 - \varphi_2$); (c) Acceleration in x -direction; (d) Acceleration in y -direction; (e) Acceleration in ψ -direction.

satisfied, the vibrating system will select one of the following three types of motion: pure circular motion, pure swing, the swing and the circular motion coexistence. The synchronization of the two excitors stems from such coupling dynamic characteristic of selecting motion. It is of great significance to design in engineering. In order to realize the feasible circular motion of the rigid frame, β should be zero and the longer l_0 .

Figure 6 shows the angle of general dynamic symmetry [19], the better the structural symmetry of system, the better the tendency that the phase difference of the two excitors approaches $-\theta_c$. By the comparison of Figs 4 and 5, we can see that $2\alpha_0$ is greatly close to $-\theta_c$ when $\beta = 0$, in other words, the structure of system is complete symmetry. Otherwise, the case is reverse.

5. Experiments

In this section, we address the validity of the simplified model and the theoretical and numerical results of the above sections, by comparing to experimental results for a laboratory model of a vibrating system.

5.1. Experiment illustration

Figure 7(a) shows the setup schematically, three acceleration sensors and two Hall-sensors are used to measure the acceleration of experimental system in x -, y - and ψ -directions and the phases of the two exciting motors, respectively. At the same time, the instantaneous phases of the two exciting motors with synchronous operation are continuously recorded by high-speed camera. Vibrating synchronization bedstand is shown in Fig. 7(b). The two exciting motors (exciters) are installed symmetrically in the main rigid body and rotating in the same directions, as shown in Fig. 7(b).

At first, it is necessary to introduce the measuring method of swinging acceleration, $\ddot{\psi}$: Two acceleration sensors are installed on the centroid position of the vibrating system (one is responsible for measuring acceleration in x -direction, the other in y -direction); the third acceleration sensor for y -direction is installed on the point A in Fig. 1, denoted by \ddot{y}_A . According to the vector mechanic analysis method, $\ddot{\psi}$ can be expressed as

$$\ddot{y}_A = \ddot{y} - l\ddot{\psi} \cos \beta_1, \quad \ddot{\psi} = (\ddot{y} - \ddot{y}_A) / (l \cos \beta_1) \quad (28)$$



Fig. 9. The phases recorded by high-speed camera before the exciter 2 is cut off ($\eta = 0.5$).

Each exciting motor has two pairs eccentric lumps which are symmetrical distribution on both ends of axis. We can adjust the included angle between two eccentric lumps to accommodate certain excited force.

The parameters of the two exciting motors are identical, model VB-326-W (380 V, 50 Hz, 6-pole, Y-connected, 0.82 A, the rated speed 950 r/min, exciting force 0~3 kN, mass 29 kG, protection grade IP54), $f_1 = f_2 = 0.002$, $\beta = 15^\circ$, $l_0 = 0.36$ m, $\xi_{nx} = 0.07$, $\xi_{ny} = 0.07$, and $\xi_{n\psi} = 0.07$, $r_l = 1.08$, $u_x = 0.97$, $u_y = 0.93$ and $u_\psi = 0.98$. The other experimental system parameters are shown in Table 2. The two exciting motors are regulated into operating with 40 Hz by converter.

5.2. Experiment results

Figure 8 shows some experimental results of the two non-excitors rotating in the same directions. Here, the masses of the two excitors are $m_1 = m_0 = 4$ kg, $m_2 = 2$ kg ($\eta = 0.5$), and their equivalent eccentric radius are same ($r = 0.053$ m). During the starting few seconds, the two excitors are supplied with the electric source at the same time, when their angular velocities pass through the resonant region of system, the two excitors excite the resonant acceleration responses in x -, y - and ψ -directions, and angular acceleration of exciter 2 is greater than that of exciter 1 since the moment of the exciter 2 (0.0056 kg·m 2) is less than that of the exciter 1 (0.0112 kg·m 2), the corresponding phase difference changed periodically, as shown in Fig. 8. Because of the damping effect, the resonant responses resulting from the starting process gradually disappear. With the time being, the two excitors reach the synchronous operation by self-adjusting of T_C , the responses of system in x -, y - and ψ -directions rapidly stabilize, the rotational velocity of synchronization nears 791 r/min and the phase difference in the steady-state nears 145°. In this case, the motion type of the rigid frame is swing and circular motion coexistence, and swing has priority because that 2α nears π . The above facts coincide with the contents in Fig. 3(b) and Table 1. When time reaches 5 s, the power supply of

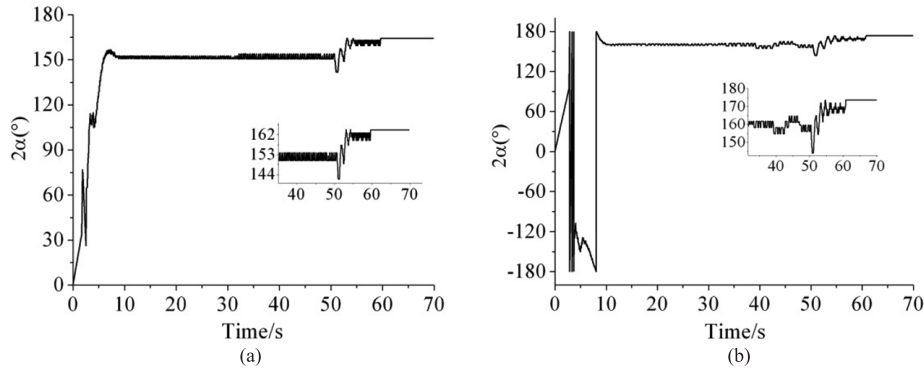


Fig. 10. The experimental results of phase difference of the two excitors rotating in the same directions for different η ($2\alpha = \varphi_1 - \varphi_2$): (a) $\eta = 1.0$; (b) $\eta = 0.8$.

the motor 2 is cut off, the phase difference decreases from 145° to 132.9° and the synchronous rotational velocity increases to 795.5 r/min, as shown in Figs 8(a) and (b). But the synchronization of the two excitors continues, this is so-called vibratory synchronization transmission [11], during which, the torque of capture, T_C transmits the driving torque from motor 1 to motor 2 to overcome the load torque of motor 2. The accelerations of $x(t)$, $y(t)$ and $\psi(t)$ are shown in the relevant figures in Fig. 8, respectively. As shown in Figs 8(a) and (b) during vibratory synchronization transmission, the stability of its synchronous state is better than that for the case before cutting off, as for the reason, is the absence of a motor's disturbance, in my opinion.

In the above experiment for $\eta = 0.5$, before exciter 2 is cut off, we recorded continuously phases of the two excitors within two cycles by high-speed camera in the steady-state, which are shown in Fig. 9. Here, high-speed camera shooting frequency is 50/s, by Fig. 9, the phase difference of the two excitors is $2\alpha = \varphi_1 - \varphi_2 \approx 143^\circ \sim 146^\circ$, which is roughly the same as that of in Figs 8(b) and 5(b) by comparing. The two excitors, hence, can operate stably and synchronously.

Figure 10 is the experimental results for $\eta = 1.0$ and $\eta = 0.8$. In Fig. 10(a), $\eta = 1.0$, the synchronous phase difference of the two excitors is $2\alpha = 152^\circ$, at 50 s, the exciter 2 is cut off, 2α increases from 152° to 164.3° ; In Fig. 10(b), $\eta = 0.8$ the synchronous phase difference is $2\alpha = 160^\circ$, at 50 s, the exciter 2 is cut off, 2α increases from 160° to 173.7° . Compared the results in Fig. 10 with that in Figs 5(c) and (d), 2α has the error of $2^\circ \sim 5^\circ$, why? Personally I think, although the models of the two motors are completely identical, electromagnetic torques of the two motors are not complete equality in practice, i.e., $T_{e01} - f_1\omega_{m0} - (T_{e02} - f_2\omega_{m0}) \neq 0$ in Eq. (13). Here, the motion type of the vibrating system in Figs 10(a) and (b) is still swing and elliptical motion coexistence.

6. Conclusions

By the theoretical investigation and experiment, the following remarks should be stressed:

With the introduction of the average method of modified small parameters, the frequency capture equation of the vibrating system is deduced. The criterion of implementing synchronization for the two excitors is derived, and that of stability of synchronous state satisfies Routh-Hurwitz criterion. These criterions can be used to evaluate and discriminate whether a self-synchronous machine used in industries is able to achieve vibratory synchronization or not, as well as to supervise the design of a self-synchronous vibrating machine has the capacity of achieving vibratory synchronization.

The regions of implementing frequency capture are presented by numeric method, as well as corresponding stabilized regions of phase difference of the two excitors.

The coupling dynamic characteristic that the vibrating system has selecting motion is discussed. Especially, in light of the case that the parameters of system are complete symmetry, the torque of frequency capture resulting from the circular motion of the rigid frame drives the phase difference to approach π and implement the swing of the rigid frame; that from the swing of the rigid frame forces the phase difference to near 0 and achieve the

circular motion of the rigid frame. When the parameters of system satisfy the criterion of stability in the regions of frequency capture, and the torque of frequency capture resulting from the circular motion is prior to that from the swing motion, the rigid frame embodies mainly the swing motion, otherwise, the circular motion. The motion of the rigid frame will be one of the following three types: pure swing, pure circular motion, swing and elliptical one coexistence. The synchronization of the two excitors stems from such dynamic characteristic of selecting motion. The corresponding motion type of the vibrating system can be achieved to meet the requirements in engineering by adjusting its structural parameters r_l , η and β . In engineering, β should near zero and l_0 as far as possible.

By the comparison of theory, numeric and experiment results, the feasibility of theory method is proved.

Acknowledgment

This work is supported by the National Natural Science Foundations of China (No. 51075063 and No. 50975045).

References

- [1] C. Huygens, *Horologium Oscillatorium*, Paris, France, 1673.
- [2] J. Rayleigh, *Theory of Sound*, Dover, New York, 1945.
- [3] B. Van der Pol, Theory of the amplitude of free and forced triode vibration, *Radio Rev* **1** (1920), 701–710.
- [4] I.I. Blekhman, *Synchronization in Science and Technology*, ASME Press, New York, 1988.
- [5] I.I. Blekhman, *Synchronization of Dynamical Systems*, Nauka, Moscow, (in Russian), 1971.
- [6] I.I. Blekhman, *Vibrational Mechanics*, World Scientific, Singapore, 2000.
- [7] I.I. Blekhman, *Selected Topics in Vibrational Mechanics*, World Scientific, Singapore, 2004
- [8] I.I. Blekhman, A.L. Fradkov, H. Nijmeijer et al., On self-synchronization and controlled synchronization, *System & Control Letters* **31** (1997), 299–305.
- [9] I.I. Blekhman, A.L. Fradkov, O.P. Tomchina et al., Self-synchronization and controlled synchronization, *Mathematics and Computers in Simulation* **58** (2002), 367–384.
- [10] I.I. Blekhman and N.P. Yaroshevich, Extension of the domain of applicability of the integral stability criterion (extremum property) in synchronization problems, *Journal of Applied Mathematics and Mechanics* **68** (2004), 839–846.
- [11] B.C. Wen, J. Fan, C.Y. Zhao et al., *Vibration Synchronization and Controlled Synchronization in Engineering*, Science Press, Beijing, 2009.
- [12] B.C. Wen, H. Zhang, S.Y. Liu et al., *Theory and Techniques of Vibrating Machinery and Their Applications*, Science Press, Beijing, 2010.
- [13] B.C. Wen, Y.N. Li and Y.M. Zhang, *Vibration Utilization Engineering*, Science Press, Beijing, (in Chinese), 2005.
- [14] B.C. Wen, Y.N. Li and Q.K. Han, *Nonlinear Vibration in Engineering*, Science Press, Beijing, (in Chinese), 2007.
- [15] B.C. Wen, Recent development of vibration utilization engineering, *Frontiers of Mechanical Engineering in China* **2**(1) (2008), 1–9.
- [16] J.M. Balthazar, J.L. Palacios Felix and R.M.L.R.F. Brasil, Short comments on self-synchronization of two non-ideal sources supported by a flexible portal frame structure, *Journal of Vibration and Control* **10** (2004), 1739–1748.
- [17] C.Y. Zhao, H.T. Zhu, R.Z. Wang et al., Synchronization of two non-identical coupled excitors in a non-resonant vibrating system of linear motion Part I: Theoretical analysis, *Shock and Vibration* **16** (2009), 505–516.
- [18] C.Y. Zhao, H.T. Zhu, T.J. Bai et al., Synchronization of two non-identical coupled excitors in a non-resonant vibrating system of linear motion Part II: Numeric analysis, *Shock and Vibration* **16** (2009), 517–528.
- [19] C.Y. Zhao, Y.M. Zhang and B.C. Wen, Synchronization and general dynamic symmetry of a vibrating system with two excitors rotating in opposite directions, *Chinese Physics B* **19** (2010), 030301.
- [20] C.Y. Zhao, H.T. Zhu, Y.M. Zhang et al., Synchronization of two coupled excitors in a vibrating system of spatial motion, *Acta Mech Sin* (2009), DOI 101007/s10409-009-0311-1.
- [21] J. Chen, *Mathematical Model and Speed Adjustment System of Alternating Motors*, Defense Press, Beijing, (in Chinese), 1989.
- [22] R.F. Nagany, *Dynamic of Synchronizing System*, Spring, Berlin, 2003.
- [23] Q.S. Lu, *Qualitative Methods and Bifurcations of Ordinary Differential Equations*, Press of Beijing, University of Aeronautics and Astronautics, Beijing, (in Chinese), 1989.
- [24] X.H. Zhang and Q.L. Zhang, *Control Theory of Nonlinear Differential Algebraic System and Its Applications*, Science Press, Beijing, (in Chinese), 2007.

